Supplemental information to: Model simulations of arctic biogeochemistry and permafrost extent are highly sensitive to the implemented snow scheme

Alexandra Pongracz, David Wårlind, Paul A. Miller and Frans-Jan W. Parmentier

S1 Adjusted respiration rate

We defined a new function following Natali et al. (2019), shown in Fig S1. The Q10 value was changed from the previous value of 200.5 to 2.9. Additionally, the minimum temperature threshold was set to -20 °C instead of the previously used -4 °C.

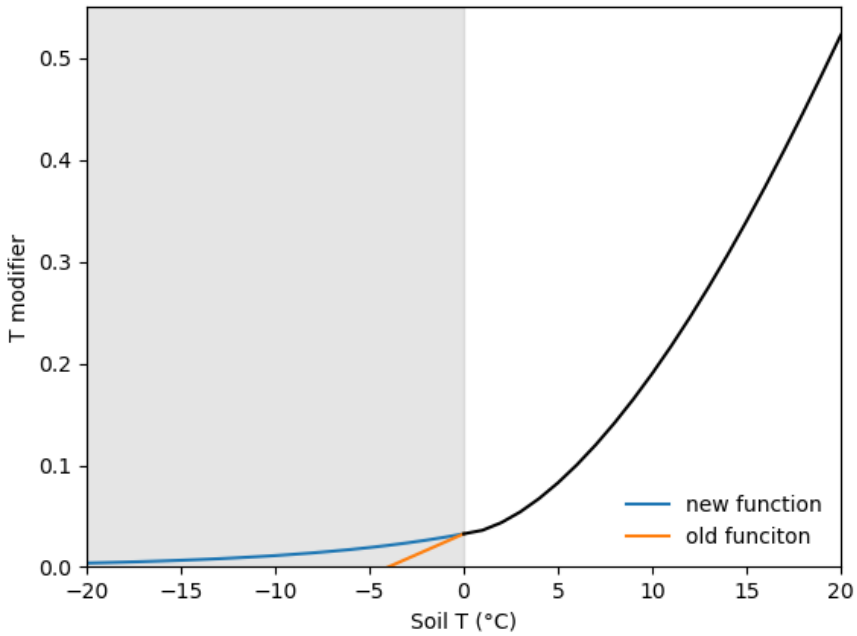

Figure S1: The old and new function controlling respiration rate during cold conditions.

S2 Site simulations

S2.1 Snowpack dynamics

Prior to the evaluation of the large-scale performance of the new, *Dynamic* snow scheme, we conducted a single-site comparison to examine the validity of the results. These detailed snow pack observations from Zackenberg helped to determine whether the *Dynamic* scheme can simulate internal snow pack dynamics, snow depth and snow density. We established the ability of the new snow scheme to simulate snow conditions by comparing a simulated snow pack with snow depth and density observations from Zackenberg (2013-2014 snow season). Figure S2 presents the observed and simulated snow pack by the *Dynamic* and *Static* schemes. This figure shows that the *Dynamic* scheme simulates higher snow depth due to lower density values in the mid and top layers of the snow pack. Density values are compared qualitatively, since it is difficult to accurately align the observational and modelled layer densities.

Thermal properties in snow layers are derived from density, and this entity is especially important in the *Dynamic* snow scheme. The comparison to observations shows that the modelled density compares well to observations. There are lower densities early in the snow season and fresh snow has a low density, while density increases in late spring during the melt season. The *Static* scheme with constant snow density simulated a somewhat higher than observed snow depth. The difference in snow depth between the *Static* and *Dynamic* simulations is small - as indicated in Fig. S2, bottom panel.

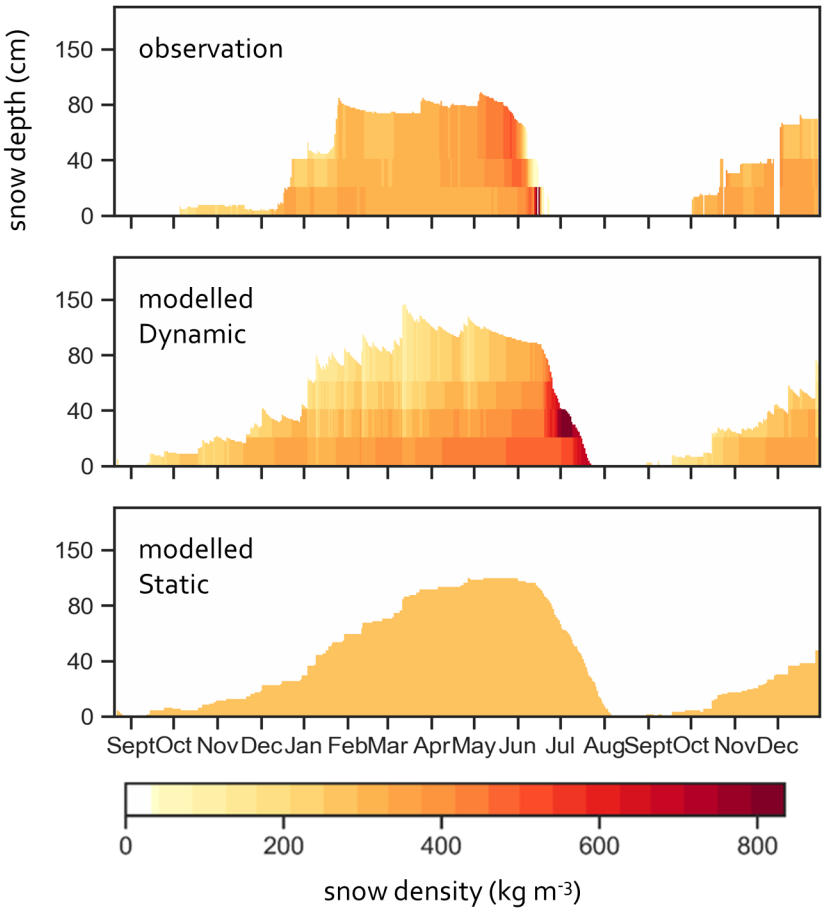

Figure S2: Snow pack dynamics at the Zackenberg GeoBasis station. Density values for the layers are extrapolated - from three and five layers for the observational and modelled data, respectively. The colours of the snow pack indicate snow density.

Overall, the new scheme reproduces the snow dynamics over the cold season better than the *Static* scheme. Please note that the model's climate forcing is a crucial controlling factor when simulating snow conditions. For this study, we used a global climate forcing dataset, which may explain some of the observed model-observation differences. Taken together, these results suggest that the *Dynamic* scheme is skilled in simulating the snow pack's internal structure and dynamics. Since the *Static* scheme has a constant snow density throughout the snow season, the *Dynamic* scheme is expected to better capture the seasonal behaviour of snow and soil conditions. The Zackenberg site comparison indicated that the *Dynamic* scheme successfully integrated these key processes affecting the density over the snow season. The mismatch between snow observations and simulations is influenced by the use of a global model forcing dataset instead of site-specific temperature, precipitation or snowfall series.

S2.2 Site simulation details

Years of observational data used for the site simulations on Abisko, Bayelva, Kytalyk, Samoylov and Zackenberg sites (PAGE21 sites) can be seen in Table S1. The computed RMSE between observed and modelled near surface soil temperature and air-soil temperature difference is shown in Table S2.

Table S1: Snow depth and near surface soil temperature data used for the site simulations, and climatic zones of the sites. (Sect.3.1)

	Abisko	Bayelva	Kytalyk	Samoylov	Zackenberg
snow depth	1986-2020	1998-2009	2011-2013	1996-2013	1996-2011
soil T	2012-2015	1998-2017	2004-2011	2012-2014	1995-2017
climatic zone	sub-arctic	high arctic	low arctic	low-arctic	high arctic

Table S2: RMSE for soil temperature and Δ T for the applied snow schemes, and temperature regimes at the Russian sites (Sect. 3.2).

		RMSE (°C)		
		-15 °C $< T_{air} <$ -5 °C	-25 °C$< T_{air} <$ -15	$T_{air} <$ -25 °C
Soil T (°C)	*Static*	6.36	12.61	18.14
	Dynamic	0.65	1.26	2.96
ΔT (°C)	*Static*	6.98	12.29	19.28
	Dynamic	1.1	0.96	3.95

S3 Pan-Arctic simulations

S3.1 Seasonal cycle of variables

Seasonal cycles of snow depth, upper soil column water content, NEE and NPP series for the *Dynamic* and *Static* simulations. Differences are calculated by subtracting the *Static* from *Dynamic* simulation outputs.

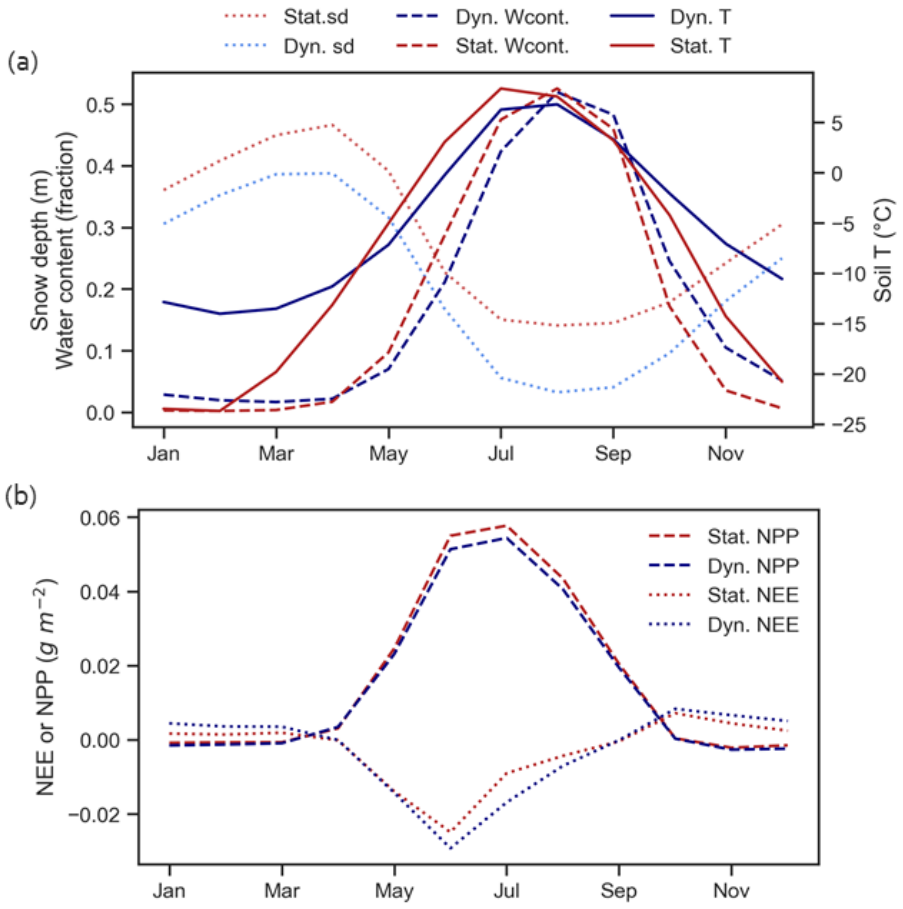

Figure S3: Seasonal dynamics of snow depth, soil temperature (25 cm depth) and fractional water content, (b) seasonal NEE and NPP.

S3.2 Simulated physical variables

These figures show the spatial pattern of simulated variables averaged over 1990-2015. Summer season values are averaged over June, July and August and winter season values are averaged over December, January and February.

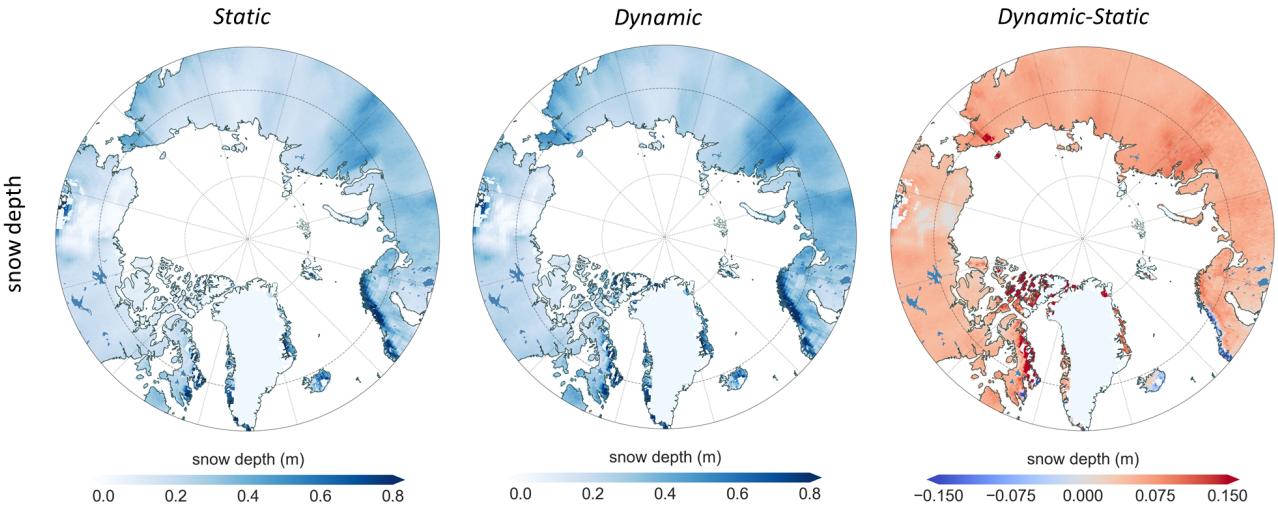

Figure S4: Simulated snow depth using the *Static* and *Dynamic* snow schemes and their difference.

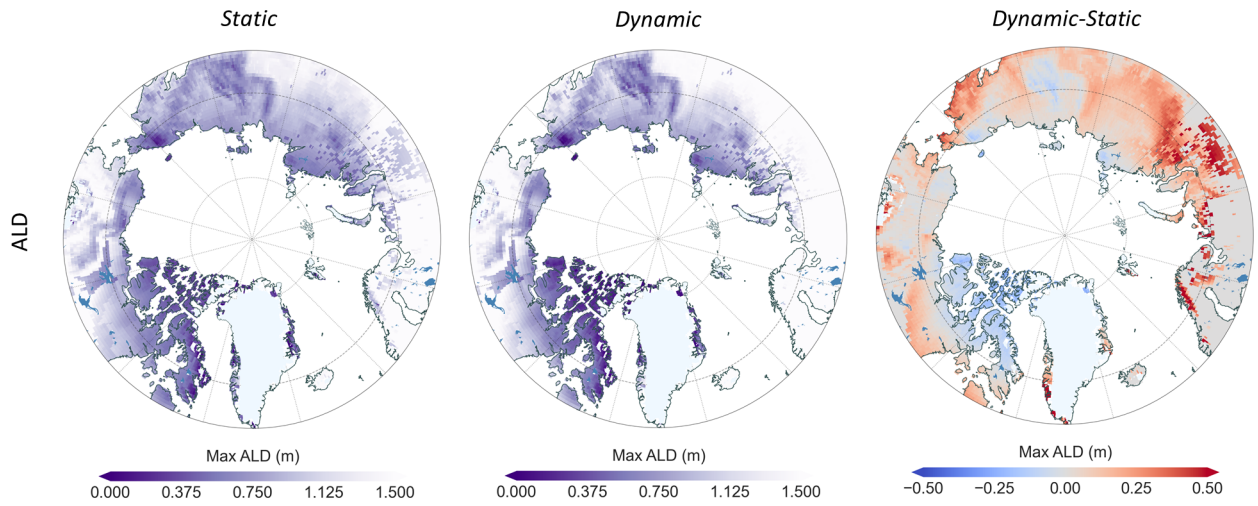

Figure S5: Simulated maximum annual active layer depth (ALD) using the *Static* and *Dynamic* snow schemes and their difference.

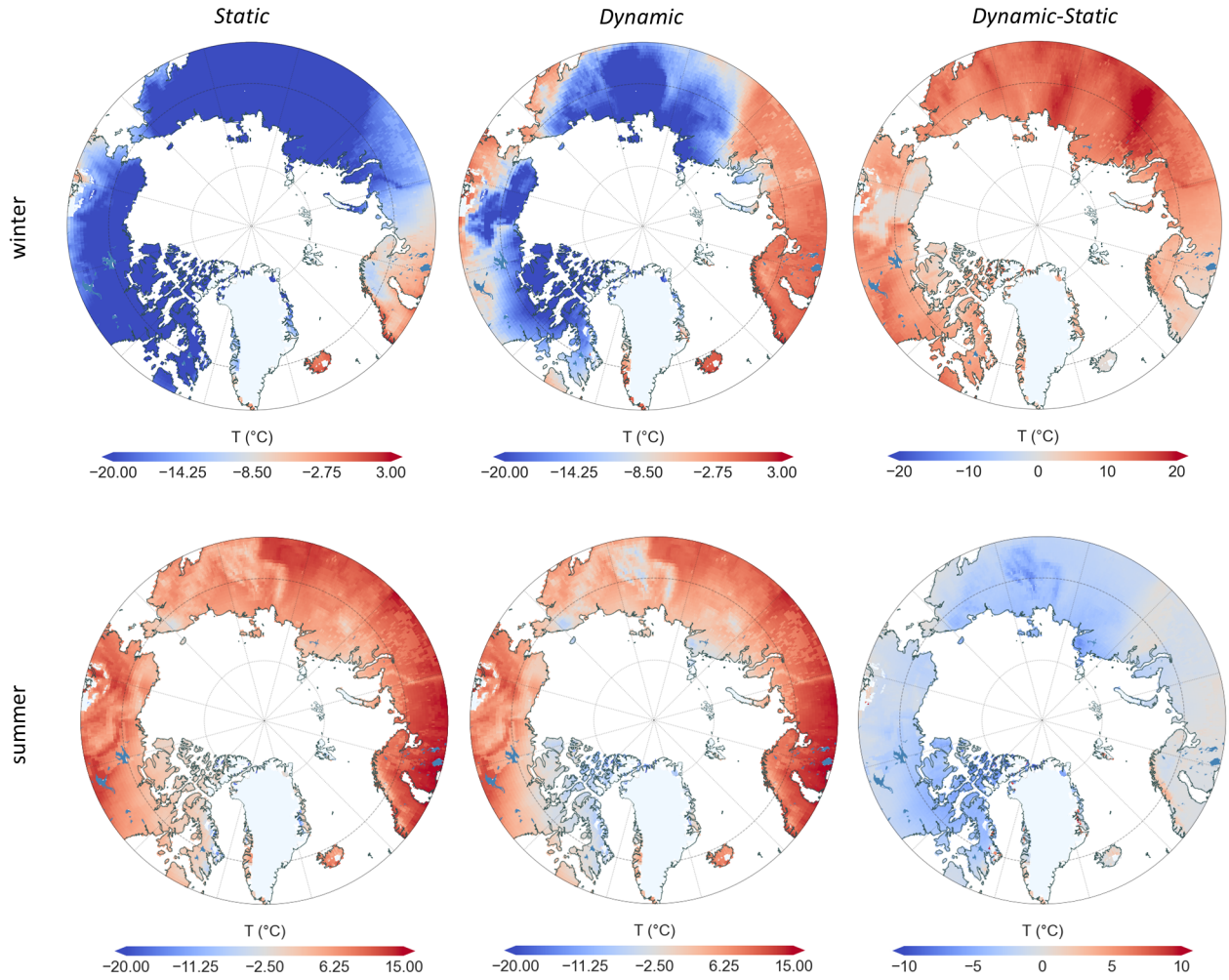

Figure S6: Simulated near surface soil temperature (25 cm depth) using the *Static* and *Dynamic* snow schemes and their difference for winter and summer.

S3.3 Simulated biogeochemical variables

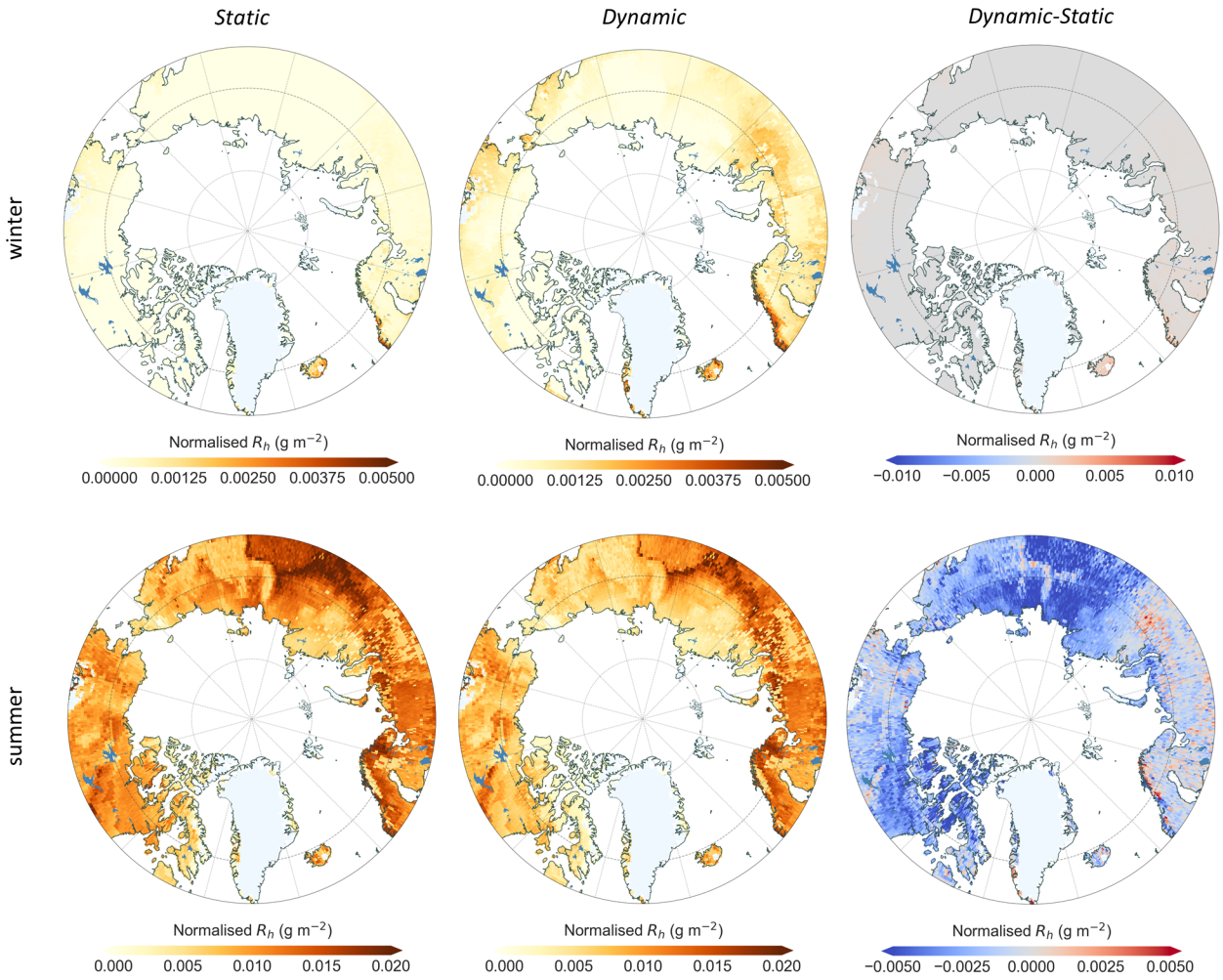

Figure S7: Simulated heterotrophic respiration normalised by soil carbon content, using the *Static* and *Dynamic* snow schemes and their difference for winter and summer.

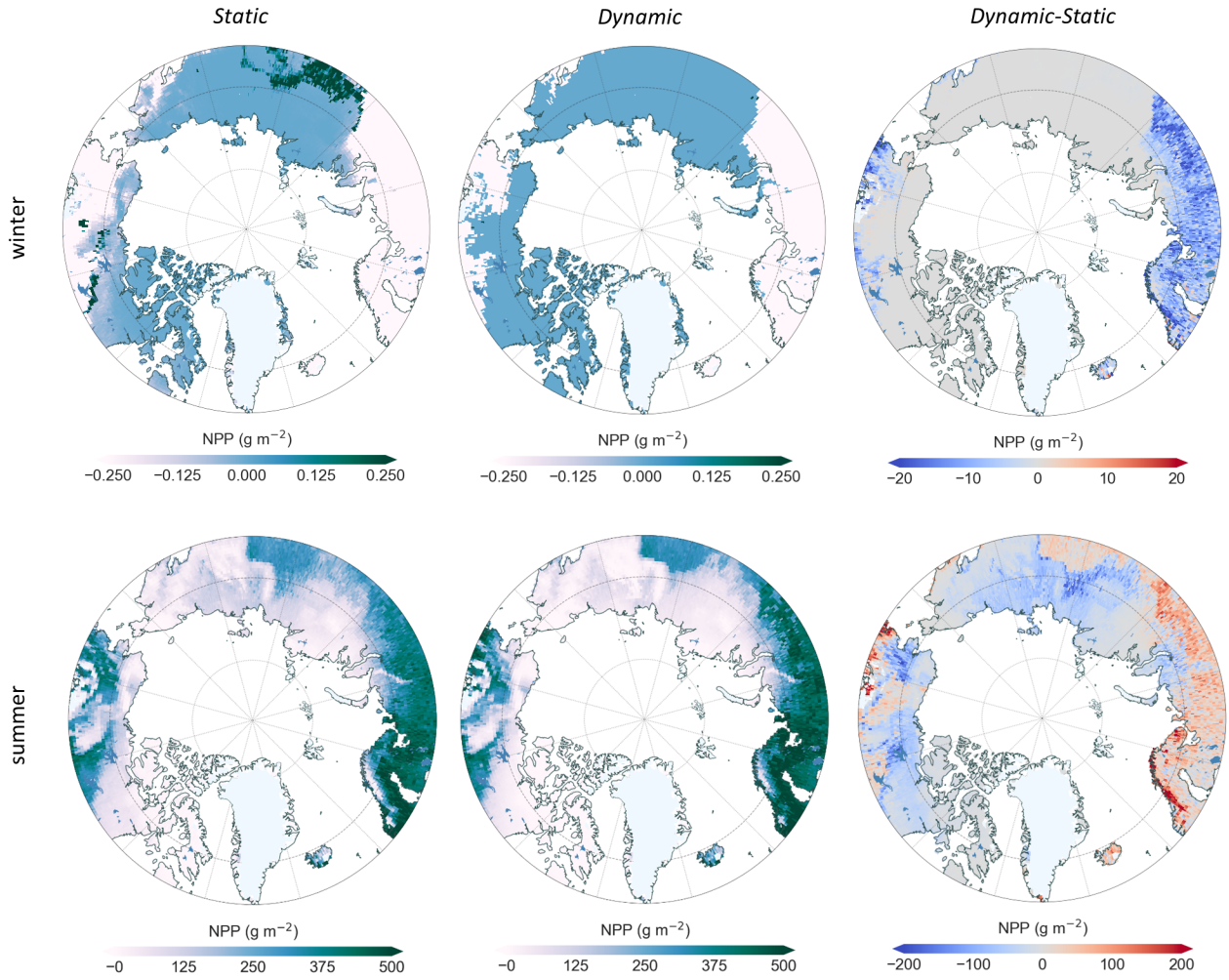

Figure S8: Simulated NPP using the *Static* and *Dynamic* snow schemes and their difference for winter and summer.

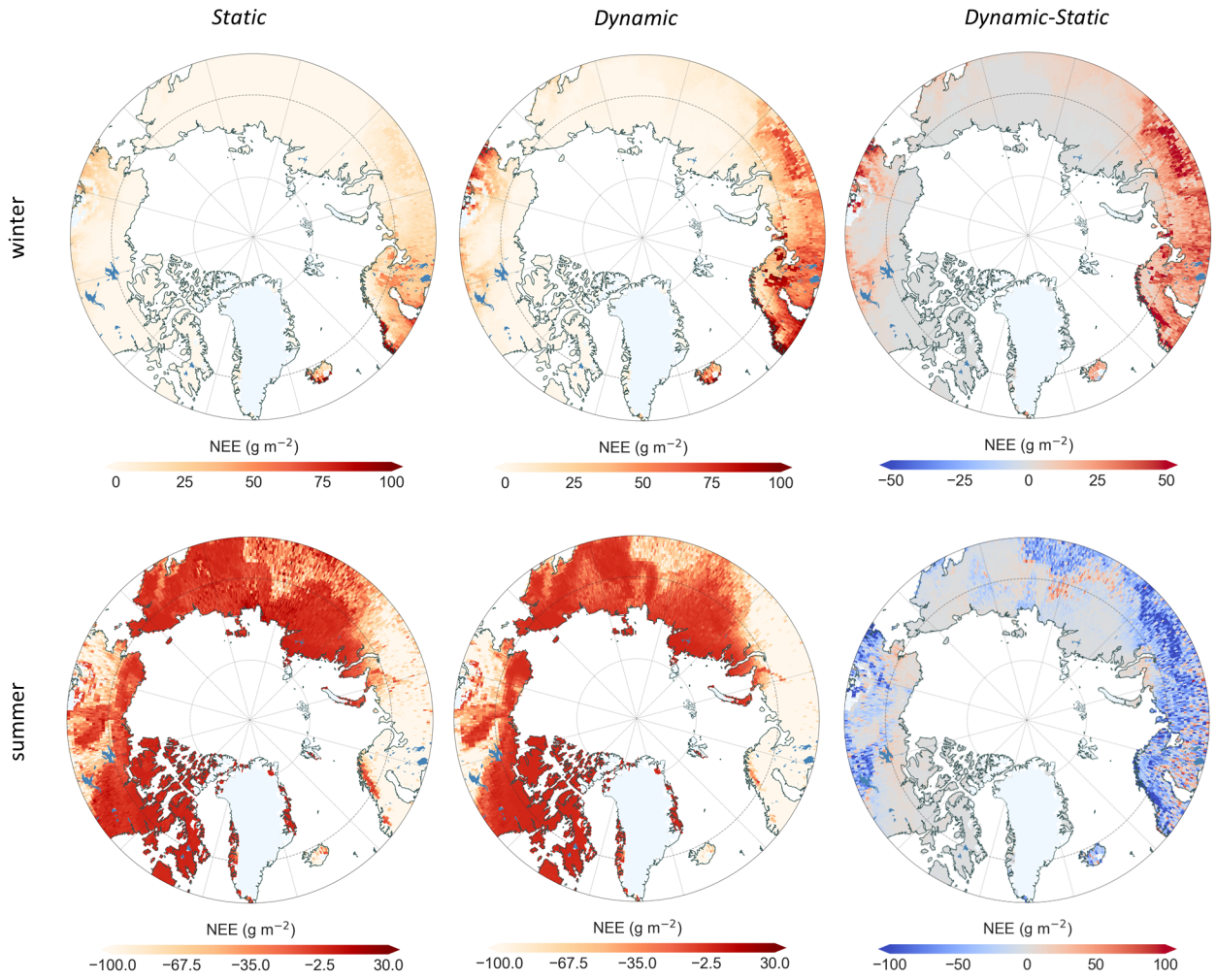

Figure S9: Simulated NEE using the *Static* and *Dynamic* snow schemes and their difference for winter and summer.

S3.4 Nitrogen cycling

Besides the carbon-related fluxes, we also assessed the impact of snow on nitrogen cycling. Figure S10 shows the nitrogen mineralisation (Fig. S10 (a)) and leaching (Fig. S10 (b)) normalised by soil carbon content. Nitrogen mineralisation only changed markedly during the summer season within the permafrost region. Leaching is higher for the *Dynamic* scheme in Eastern-Canada and Northern-Russia. Nitrogen use efficiency (NUE) on panel (c) was calculated as the ratio between NPP and nitrogen uptake. The *Dynamic* scheme simulates a lower NUE than the Static scheme, which indicates a higher N uptake per unit productivity.

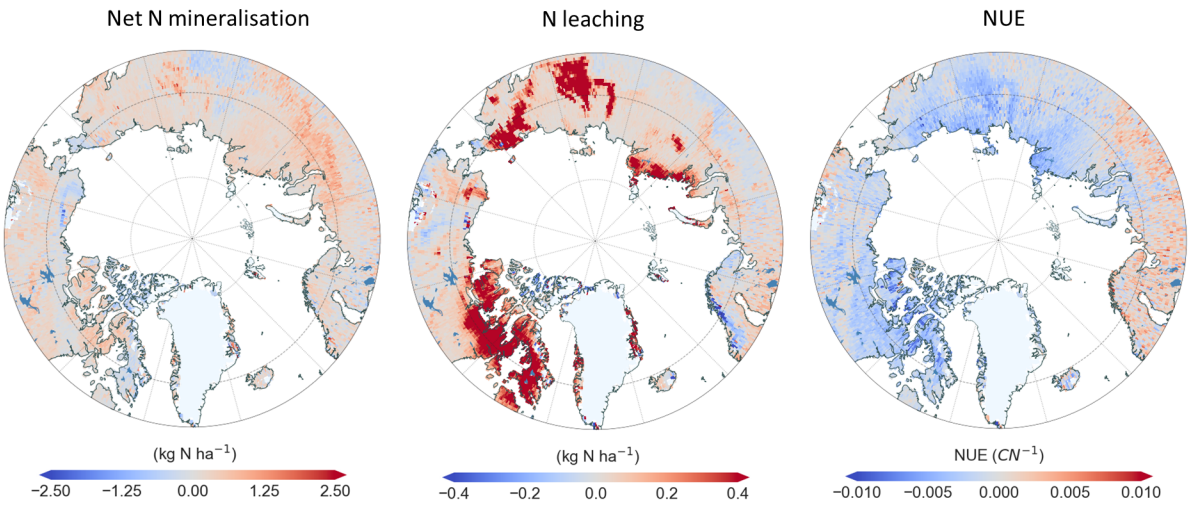

Figure S10: Nitrogen mineralisation, N leaching and NUE difference calculated by by subtracting the *Static* from *Dynamic* simulation outputs.

Table S3: Pan-arctic mean values for the studied variables for the *Static* and *Dynamic* simulations, and their respective differences.

variable	unit	*Static*	*Dynamic*	*Dynamic-Static*	note of changes
$snowdepth$	m	0.22	0.3	0.06	general increase
ALD	m	0.98	1.05	0.07	increase in ALD
$soilT_{winter}$	°C	-22.6	-12.5	10.16	increased in T
$soilT_{summer}$	°C	6.3	4.3	-2.0	decrease in T
GPP_{winter}	g m^{-2}	0.14	0.2	0.04	increase in gross production
GPP_{summer}	g m^{-2}	221.1	211.6	-9.4	decrease in gross production
NPP_{winter}	g m^{-2}	-3.0	-5.2	-2.1	decrease in productivity
NPP_{summer}	g m^{-2}	156.2	146.3	-9.8	decrease in productivity
Rh_{winter}	g m^{-2}	2.5	7.7	5.3	increase in R_h
Rh_{summer}	g m^{-2}	116.8	93.1	-24.7	decrease in R_h
NEE_{winter}	g m^{-2}	5.5	13.0	7.4	increased carbon emission
NEE_{summer}	g m^{-2}	-38.3	-53.2	-14.9	increased carbon uptake
$soilC$	kg C m^{-2}	11.1	10.2	-0.97	decrease in soil C
$vegC$	kg C m^{-2}	1.9	1.9	0.06	marginal difference

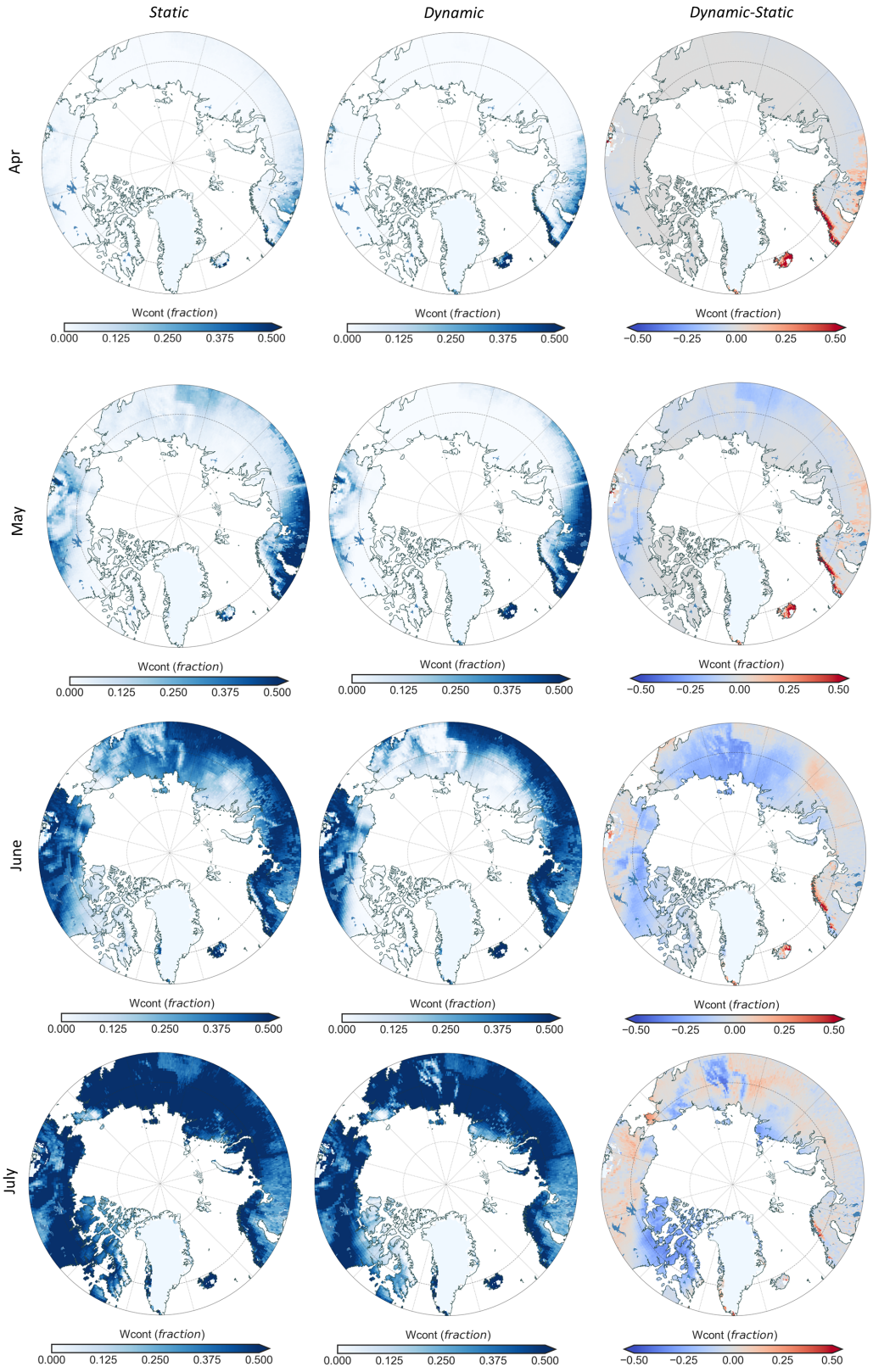

Figure S11: Mean fractional water content of the upper soil column in April, May, June and July, using the *Static*, *Dynamic* schemes and their difference.

S3.5 Vegetation dynamics

Sites where PFT dominance changed between the *Static* and *Dynamic* simulations is shown in Fig. **??**. These transition sites are scattered across the Arctic, but there are some clear hotspots in Eastern-Russia, the Scandinavian coastline and Northern-America.

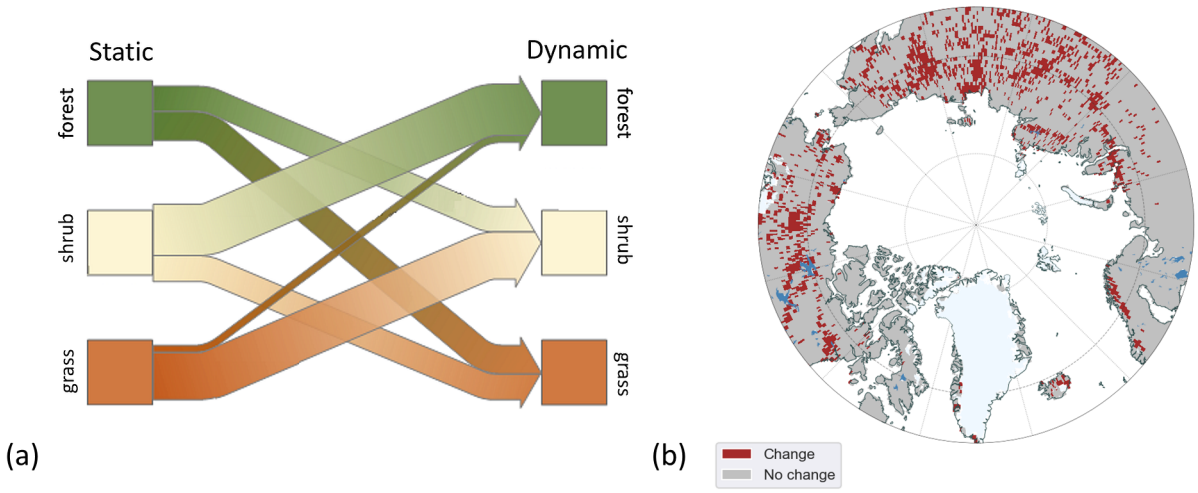

Figure S12: (a) Direction of dominant vegetation group changes between the *Static* and *Dynamic* schemes. The size of arrows show the number of sites transitioning. (b) Spatial distribution of sites where PFT dominance changed between the simulations.

References

Natali, S. M., Watts, J. D., Rogers, B. M., Potter, S., Ludwig, S. M., Selbmann, A.-K., Sullivan, P. F., Abbott, B. W., Arndt, K. A., Birch, L., Bjorkman, M. P., Bloom, A. A., Celis, G., Christensen, T. R., Christiansen, C. T., Commane, R., Cooper, E. J., Crill, P., Czimczik, C., Davydov, S., Du, J., Egan, J. E., Elberling, B., Euskirchen, E. S., Friborg, T., Genet, H., Göckede, M., Goodrich, J. P., Grogan, P., Helbig, M., Jafarov, E. E., Jastrow, J. D., Kalhori, A. A. M., Kim, Y., Kimball, J. S., Kutzbach, L., Lara, M. J., Larsen, K. S., Lee, B.-Y., Liu, Z., Loranty, M. M., Lund, M., Lupascu, M., Madani, N., Malhotra, A., Matamala, R., McFarland, J., McGuire, A. D., Michelsen, A., Minions, C., Oechel, W. C., Olefeldt, D., Parmentier, F.-J. W., Pirk, N., Poulter, B., Quinton, W., Rezanezhad, F., Risk, D., Sachs, T., Schaefer, K., Schmidt, N. M., Schuur, E. A. G., Semenchuk, P. R., Shaver, G., Sonnentag, O., Starr, G., Treat, C. C., Waldrop, M. P., Wang, Y., Welker, J., Wille, C., Xu, X., Zhang, Z., Zhuang, Q. & Zona, D. (2019), 'Large loss of co2 in winter observed across the northern permafrost region', Nature Climate Change **9**(11).